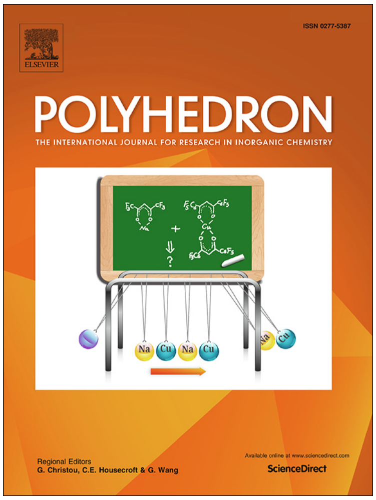

Core-shell structured magnetic mesoporous silica-titania: A novel, powerful and recoverable nanocatalyst

Marziyeh Vahidian, Dawood Elhamifar, Masoumeh Shaker

PII: S0277-5387(19)30771-5
DOI: https://doi.org/10.1016/j.poly.2019.114326
Reference: POLY 114326

To appear in: *Polyhedron*

Received Date: 6 August 2019
Revised Date: 22 November 2019
Accepted Date: 19 December 2019

Please cite this article as: M. Vahidian, D. Elhamifar, M. Shaker, Core-shell structured magnetic mesoporous silica-titania: A novel, powerful and recoverable nanocatalyst, *Polyhedron* (2019), doi: https://doi.org/10.1016/j.poly.2019.114326

Core-shell structured magnetic mesoporous silica-titania: A novel, powerful and recoverable nanocatalyst

Marziyeh Vahidian, Dawood Elhamifar* and Masoumeh Shaker

Department of Chemistry, Yasouj University, Yasouj, 75918-74831, Iran

E-mail: d.elhamifar@yu.ac.ir

Abstract: In this research, a novel core-shell nanostructured magnetic Ti-silica (Mag@MCM-41/TiO_2) is synthesized, characterized and its catalytic application is investigated in the production of 1-(α-aminoalkyl)-2-naphthols. The Mag@MCM-41/TiO_2 was prepared *via* surfactant directed hydrolysis and co-condensation of tetramethoxysilane (TMOS) around Mag@SiO_2 NPs followed by treatment with tetrabutylorthotitanate ($Ti(O^tBu)_4$). The Mag@MCM-41/TiO_2 catalyst was characterized using VSM, FTIR, EDX, SEM, TEM and PXRD. The Mag@MCM-41/TiO_2 was applied as an efficient catalyst in the synthesis of 1-(α-aminoalkyl)-2-naphthols under ultrasonic conditions at 50 °C. This nanocatalyst was recovered and reused for several times under applied conditions.

Keywords: Core-shell nanostructure, Magnetic Ti-silica, 1-(α-aminoalkyl)-2-naphthols, Ultrasonic conditions, Nanocatalyst

1. Introduction

Over the past few decades, the synthesis of magnetic nanoparticles has been the subject of extensive research. Among the magnetic nanoparticles, iron oxides are highly regarded in scientific and technological terms due to their optical, electrical, magnetic, and catalytic properties [1]. These NPs and their nanocomposites are widely used in various fields such as gas sensors [2], information storage devices [3], catalysis [4, 5], adsorbent materials [6], pigments [7], water purification [8], magnetic resonance imaging (MRI) [9-11], hyperthermia treatment [12], tissue repair [13], detoxification of biological fluids [14], labeling and separation of cells [15, 16], drug delivery [17-19] and biological sensors [20]. Up to now, 16 pure phases of iron oxides including oxides, hydroxides and oxyhydroxides, have been identified. Among these, magnetite (Fe_3O_4) offers the most interesting magnetic and electron properties due to the presence of iron cations in both capacities (Fe^{2+}, Fe^{3+}). In comparison with other materials, magnetite NPs are of great interest to researchers due to their proper biocompatibility, non-toxicity, strong superparamagnetic properties and easy preparation [13, 21-23]. However, Fe_3O_4 NPs tend to self-assembly due to their large surface area, high surface energy, magnetic properties and hydrophilic surfaces [24]. To solve these problems many studies are focused on the modification of Fe_3O_4 NPs surface with different organic and inorganic materials to form magnetic core-shell structures [25]. Due to its unique properties, silica is the most common mineral substance to modify the surface of the magnetic MNPs. Magnetic mesoporous silicas are very attracted between chemists due to they have advantages of both MNPs and mesostructures such as simple recoverability, high surface area and easy modification of their surface with different catalysts [26-28]. To date several magnetic nanosilica supported catalysts have been prepared and their applications have been studied in chemical processes [29-34]. Some of recently reported materials are Fe_3O_4@MCM-41-Im@MnPor [29], Fe_3O_4@MCM-41@Pd-SPATB [30], Rd-MCM-41@Fe_3O_4 [31], $Yb(OTf)_2$-SO_3Na&Ph-MCMSS [32] and Fe_3O_4@MCM-41-SH [33].

On the other hand, multi-component reactions have been considered and developed as an effective and helpful way for the synthesis of fine organic compounds. One of these important processes is Betti reaction producing amino-naphthol products (or Betti bases) that are very attractive between chemists due to their pharmacological properties such as blood pressure reducer, anti-cancer, heart beat, anti-bacterial, antipain and selective estrogen receptors. Also, the non-racemic aminonaphthols are as valuable chiral ligands or chiral auxiliaries in asymmetric synthesis. [35-38]. The starting materials used for Betti reaction are primary and secondary aliphatic or aromatic amines, aliphatic and aromatic aldehydes, phenols and β-naphthols (Scheme 1). This reaction has been performed under both homogeneous and heterogeneous conditions in the presence of different catalysts such as nanocrystalline MgO [35], $Cu(OTf)_2.SiO_2$ [36], spherical Fe_3O_4 MNPs [37], reverse ZnO nanomicelles [39], rMGO-Au NPs composite [40], Triton X-100 [38], nano-SiO_2–H_3BO_3 [41], ChPS TSIL [42], triflic acids [43], $[Et_3N–SO_3H]Cl$ [44], Sodium dodecyl sulfate (SDS) [45].

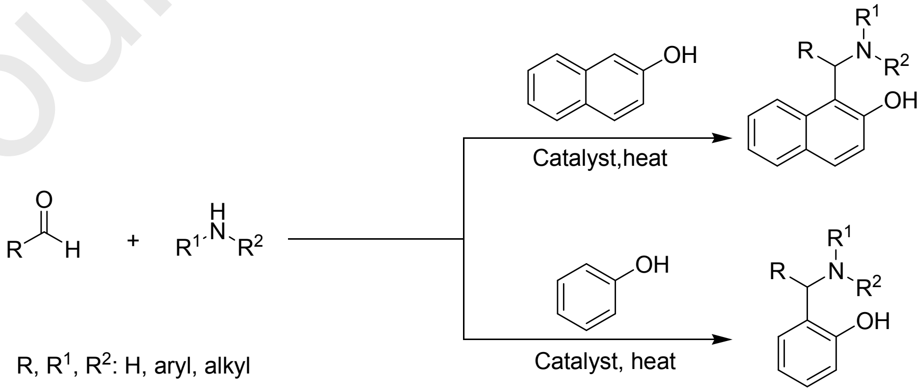

Scheme 1. The Betti reaction

Herein, synthesis and characterization of a novel magnetic mesoporous Ti-silica (Mag@MCM-41/TiO_2) with core-shell structure are developed. Moreover, the catalytic application of Mag@MCM-41/TiO_2 is studied in the Betti reaction to produce 1-(α-aminoalkyl)-2-naphthols (Scheme 2).

2. Experimental Section

2. 1. General

All chemicals and reagents such as iron (II) chloride tetrahydrate (99%), iron (III) chloride hexahydrate (99%), cetyltrimethylammonium bromide (CTAB, 98%), ammonia (NH_3, 25% wt), tetramethoxysilane (TMOS, 99%), tetrabutylorthotitanate ($[Ti(OtBu)_4]$, 97%), 2–naphthol and all applied aldehydes and amines were purchased from Sigma-Aldrich, Merck and Fluka companies. The reaction progress was monitored using TLC. The morphology of the particles was evaluated by Philips, XL30 emission scanning electron microscope (SEM). Fourier transform infrared (FT-IR) spectroscopy was recorded on a Brucker-Vector 22 spectrometer. Powder X-ray diffraction (PXRD) was obtained using a Panalytical X-Pert diffractometer. The magnetic properties of the particles were investigated using vibrating sample magnetometer (VSM) of Meghnatis Daghigh Kavir Company. Energy-dispersive X-ray spectroscopy (EDX) was obtained by TESCAN Vega Model. Melting points were determined using a KSB1N, Kruss apparatus in open capillary tubes. Ultrasonic model KMM1-120WE301 was used to disperse the particles and to perform the organic reactions. ^{1}HNMR and ^{13}CNMR spectra were recorded in DMSO solvent using a Bruker Advanced DMX-400 MHz spectrometer.

2.2. Synthesis of Mag@MCM-41/TiO_2

For the synthesis of Mag@MCM-41/TiO_2, firstly the Fe_3O_4 and Mag@SiO_2 nanoparticles were prepared according to reported procedures [46, 47]. To prepare the Mag@MCM-41 nanoparticles, Mag@SiO_2 nanospheres (0.6 g) were first ultrasonically dispersed in deoxygenated water (60 mL) for 0.5 h under argon atmosphere. Then, cetyltrimethylammonium bromide (CTAB, 1 g) and NH_3 (25% wt, 3 mL) were added and the mixture was stirred mechanically at 25 ºC. After that, 0.7 mL of TMOS was drop-wise added and stirring was continued at same temperature for 2 h under argon atmosphere. Next, the obtained combination was statically heated during 48 h at 100 °C. The product was collected using an external magnet, washed completely with EtOH and dried for 6 h at 70 °C. The cetyltrimethylammonium bromide (CTAB) surfactant was eliminated by calcination at 500 °C for 6 h and the obtained powder was called Mag@MCM-41. Finally, the Mag@MCM-41 (0.5 g) was stirred in 40 mL of deoxygenated DMSO and concurrently 1 mL of tetrabutylorthotitanate [$Ti(O^tBu)_4$] was added drop-wise at room temperature under argon atmosphere. After 2 h stirring, the final product was isolated, washed with EtOH, dried at 80 ºC for 10 h and called Mag@MCM-41/TiO_2 nanocatalyst. The loading of titanium onto/into material framework was calculated based on ICP and EDX results (4.56 mmol Ti/gram of material).

2.3. Synthesis of 1-(α-aminoalkyl)-2-naphthols using Mag@MCM-41/TiO_2 catalyst

For this, 1 mmol of 2–naphthol, 1 mmol of aldehyde, 1 mmol of amine and catalyst Mag@MCM-41/TiO_2 (2.3 mol%) were added in a reaction flask and this mixture was heated at 50 °C under ultrasonic irradiations. After completion of the process, monitored by TLC, 10 mL of ethyl acetate was added and the Mag@MCM-41/TiO_2 was removed *via* a magnetic field. Finally, the solvent was evaporated and pure products were obtained after recrystallization in ethanol. The products were characterized using NMR and IR spectroscopies. It is important to note that in this process, the 2–naphthol was limiting reagent. For performing reaction in an oil bath, the above mentioned amounts of starting materials and catalyst were added in a flask while stirring at 50 °C in an oil bath. After completing of the process, the pure product was obtained as above.

2.4. Procedure for the recovery of Fe_3O_4@MCM-41/TiO_2 nanocatalyst

For this, the reaction between benzaldehyde, 2–naphthol and pipiridine in the presence of designed catalyst was selected as a reaction model under optimized reaction. The reaction progress was monitored by TLC. After finishing of the reaction, ethyl acetate (10 mL) was added in reaction vessel and catalyst was removed using an external magnet. The catalyst was washed with ethanol and dried at 80 ºC. The recovered catalyst was reused in the next run under conditions as the first run. These steps were repeated several times and the yield of each run was calculated and reported.

2.5. The IR and NMR data of some Betti products are as following

2.5.1. 1-((4-Bromophenyl)(piperidin-1-yl)methyl)naphthalen-2-ol

White solid; yield: 0.371g, 94 %; mp: 159-161 ºC [48]; IR (KBr, cm^{-1}): 3328 (O-H), 3080 (=C-H, stretching vibration, sp^2), 2939 (C-H stretching vibration, sp^3), 1508-1624 (C=C, Ar), 1234 (C-N), 749 (C-Br). ^1H NMR (DMSO, 400 MHz) ↗ (ppm):□1.47 (s, 2H), 1.58 (s, 4H), 2.37(s, 4H), 5.34 (s, 1H), 7.09 (d, *J*= 8.8 Hz, 1H,), 7.25 (t, *J*= 7.6, 1H), 7.40 (t, *J*□ 7.6 Hz,1H), 7.51 (d, *J*= 8 Hz, 2H), 7.58 (d, *J*= 7.6 Hz, 2H), 7.72 (d, *J*= 6.4 Hz,1H), 7.76 (d, *J*= 8.4 Hz, 1H), 8.01 (d, *J*= 8 Hz,1H), 13.73(s, 1H, OH). ^{13}C NMR (CDCl$_3$, 100 MHz) δ (ppm): 24.0, 26.0, 52.7, 69.6, 116.5, 120.1, 121.3, 121.7, 122.9, 127.0, 128.49, 128.59, 128.5, 129.1, 129.7, 131.2, 132.1, 132.3, 141.1, 155.5.

2.5.2. 1-((2-Chlorophenyl)(piperidin-1-yl)methyl)naphthalen-2-ol

White solid; yield: 0.309g, 88 %; mp: 136-138 ºC [48]; IR (KBr, cm^{-1}): 3331 (O-H), 3065 (=C-H, stretching vibration, sp^2), 2977 (C-H stretching vibration, sp^3), 1510-1657 (C=C, Ar), 1230 (C-N), 753 (C-Cl).

2.5.3. 1-(Phenyl(piperidin-1-yl)methyl)naphthalen-2-ol

White solid; yield: 0.301g, 95 %; mp: 195-196 ºC [49]; IR (KBr, cm^{-1}): 3311 (O-H), 3073 (=C-H, stretching vibration, sp^2), 2947 (C-H stretching vibration, sp^3), 1503-1641 (C=C, Ar), 1238 (C-N).

2.5.4. 1-(Piperidin-1-yl(p-tolyl)methyl)naphthalen-2-ol

White solid; yield: 0.278g, 84 %; mp: 144-146 ºC [49]; IR (KBr, cm^{-1}): 3396 (O-H), 3064 (=C-H, stretching vibration, sp^2), 2963 (C-H stretching vibration, sp^3), 1508-1657(C=C, Ar), 1231 (C-N).

2.5.5. 1-((2-Nitrophenyl)(piperidin-1-yl)methyl)naphthalen-2-ol

Yellow solid; yield: 0.347g, 96 %; mp: 196-198 ºC [49]; IR (KBr, cm^{-1}): 3354 (O-H), 3024 (=C-H, stretching vibration, sp^2), 2931 (C-H stretching vibration, sp^3), 1508-1657(C=C, Ar), 1564 and 1342 (NO$_2$), 1240 (C-N).

2.5.6. 1-((2-Nitrophenyl)(phenylamino)methyl)naphthalen)-2-ol

Yellow solid; yield: 0.333g, 90 %; mp: 132-134 ºC [39]; IR (KBr, cm^{-1}): 3412 (N-H), 3363 (O-H), 3008 (=C-H, stretching vibration, sp^2), 2947 (C-H stretching vibration, sp^3), 1510-1642(C=C, Ar), 1584 and 1372 (NO_2), 1235 (C-N).

2.5.7. 1-((Phenyl)(butylamino)methyl)naphthalen-2-ol

White solid; yield: 0.286g, 94 %; mp: 130-132 ºC [40]; IR (KBr, cm^{-1}): 3442 (N-H), 3300 (O-H), 3014 (=C-H, stretching vibration, sp^2), 2937 (C-H stretching vibration, sp^3), 1503-1641 (C=C, Ar), 1238 (C-N).

3. Results and discussion

To prepare Mag@MCM-41/TiO_2, the Fe_3O_4@SiO_2 core-shell nanoparticles were firstly prepared according to a well-known procedure [46, 47]. Secondly, the magnetic mesoporous Mag@MCM-41 nanocomposite was prepared through hydrolysis and condensation of TMOS around Mag@SiO_2 nanoparticles in the presence of CTAB surfactant under alkaline conditions. After calcination to remove CTAB, the Mag@MCM-41 was treated with tetrabutylorthotitanate [$Ti(O^tBu)_4$] to deliver desired Mag@MCM-41/TiO_2 catalyst (Scheme 2). The structural and chemical properties of the Mag@MCM-41/TiO_2 nanocatalyst were investigated using FT-IR, SEM, TEM, EDX, PXRD and VSM.

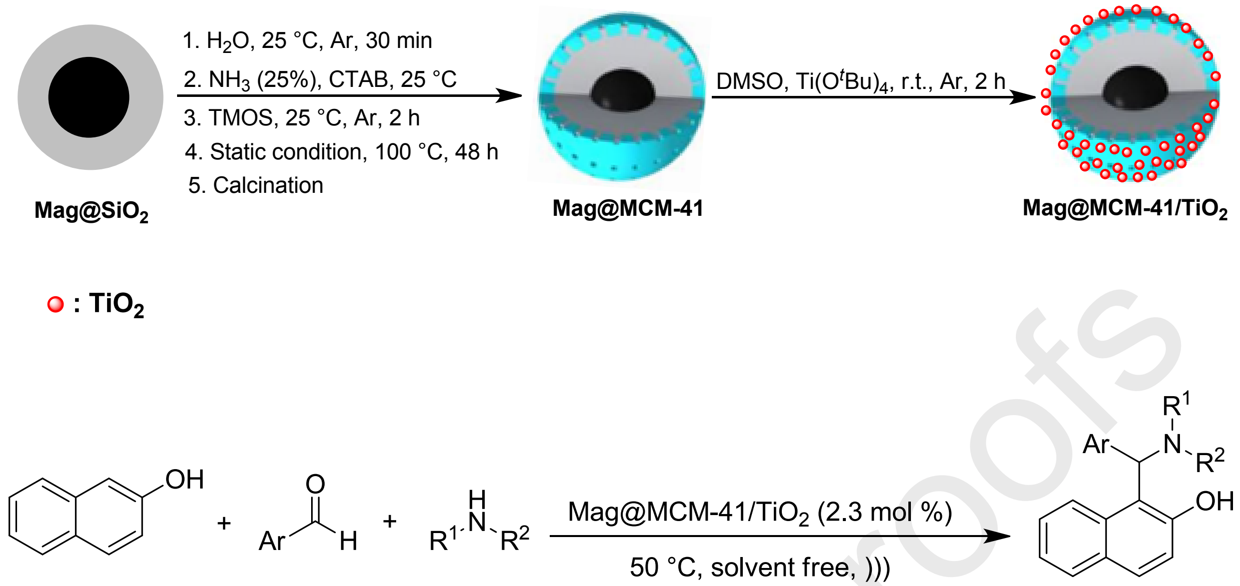

Scheme 2. Synthesis of Mag@MCM-41/TiO$_2$ and its catalytic application in Betti reaction

The FT-IR of Fe$_3$O$_4$ (Fig. 1 a) showed two peaks at 559 and 3419 cm^{-1} corresponding to the Fe-O and O-H bonds, respectively. For Mag@MCM-41 (Fig. 1 b) and Mag@MCM-41/TiO$_2$ (Fig. 1 c), the signals of Si-O-Si bonds were appeared at 1050 and 955 cm^{-1}. Also for the latter samples, the peak observed at 3419 cm^{-1} is related to stretching vibration of O-H bond. Moreover, the band cleared at 1632 cm^{-1} is due to bending vibration of O–H bonds. The broad signals in the absorption range of 500-900 and 940–960 cm^{-1} are assigned to Ti-O-Ti and Ti-O-Si bonds, respectively (Fig. 1) [50]. In fact, the successful immobilization of titanium oxide particles on the surface of Mag@MCM-41 is confirmed by this analysis.

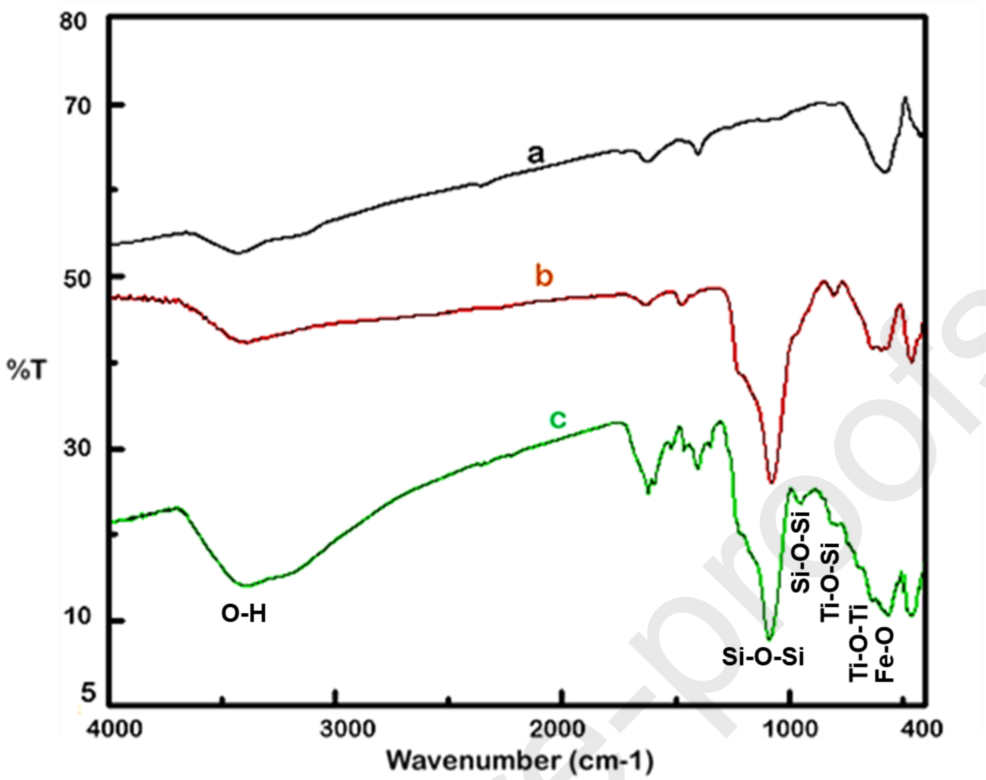

Fig. 1. FT-IR spectra of a) Fe_3O_4, b) Mag@MCM-41 and c) Mag@MCM-41/TiO_2 materials

The PXRD analysis of the Fe_3O_4 and Mag@MCM-41/TiO_2 (Fig. 2) showed the same pattern with six reflection peaks at 2θ of 63.41, 57.56, 54.10, 43.92, 36.01 and 30.38 degrees, corresponding to the Miller indices values (*hkl*) of 440, 511, 422, 400, 311 and 220, respectively, proving that the crystalline structure of the magnetite NPs is maintained during the catalyst preparation steps [2, 6].

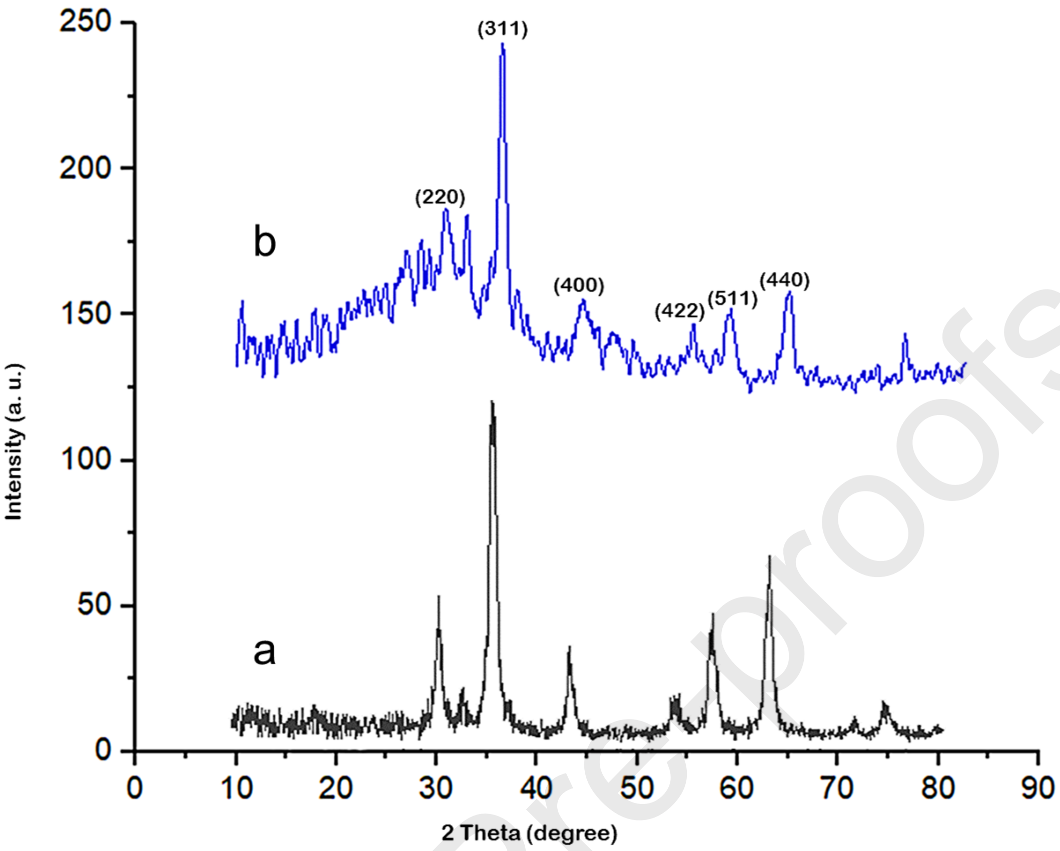

Fig. 2. PXRD pattern of the a) Fe_3O_4 and b) Mag@MCM-41/TiO_2 nanomaterials

The expected composition of Mag@MCM-41/TiO_2 was studied by EDX spectroscopy. As shown, the peaks of titanium, iron, silicon and oxygen are observed in the EDX spectrum confirming successful coating of silica-titania species onto iron oxide particles (Fig. 3). Worth noting that quantitative determination of the elements was also performed using EDX analysis that for Ti, Fe, Si and O this was 21.84 %, 58.70 %, 7.11 % and 12.36 %, respectively.

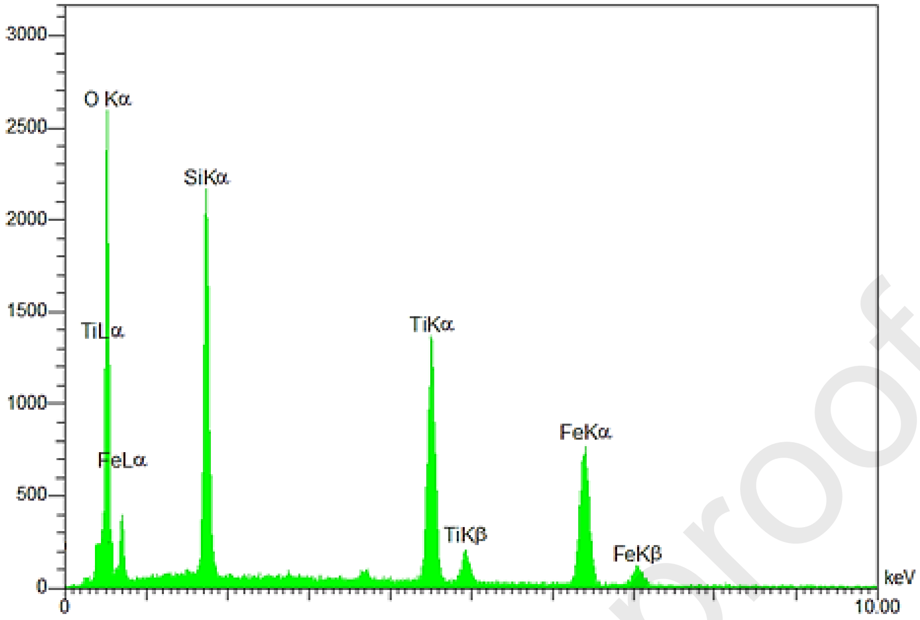

Fig. 3. EDX analysis of the Mag@MCM-41/TiO_2 nanocatalyst

The SEM analysis showed the presence of particles with spherical morphology and average size of 70 nm for the Mag@MCM-41/TiO_2 nanocatalyst (Fig. 4). The TEM image (Fig. 5) also showed a core-shell stricture for the material with black core (magnetite NPs) and gray shell (MCM-41/TiO_2 layer).

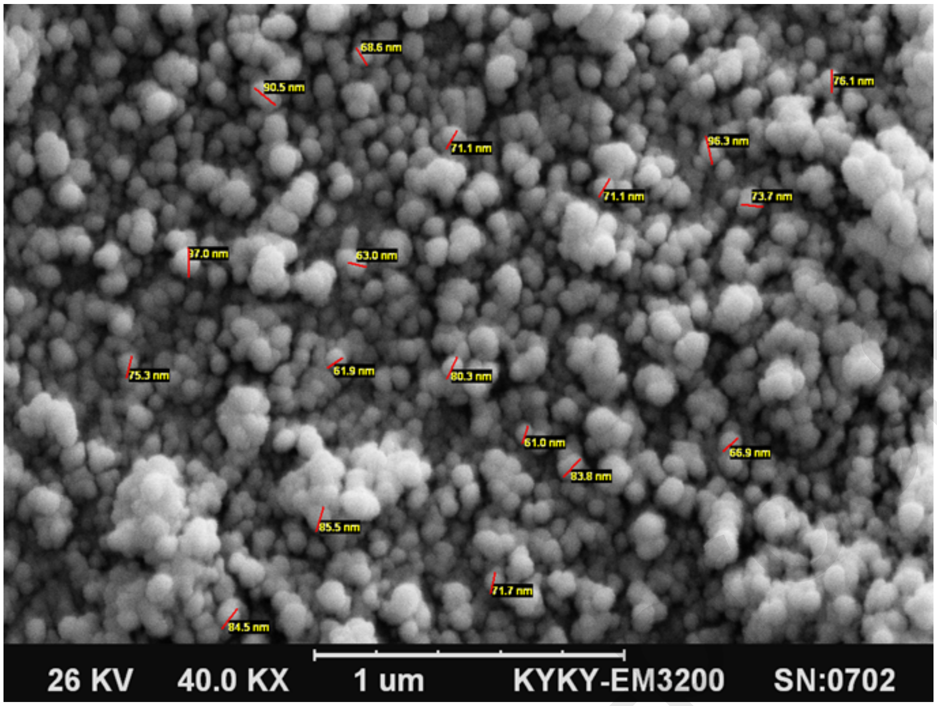

Fig. 4. SEM analysis of Mag@MCM-41/TiO_2

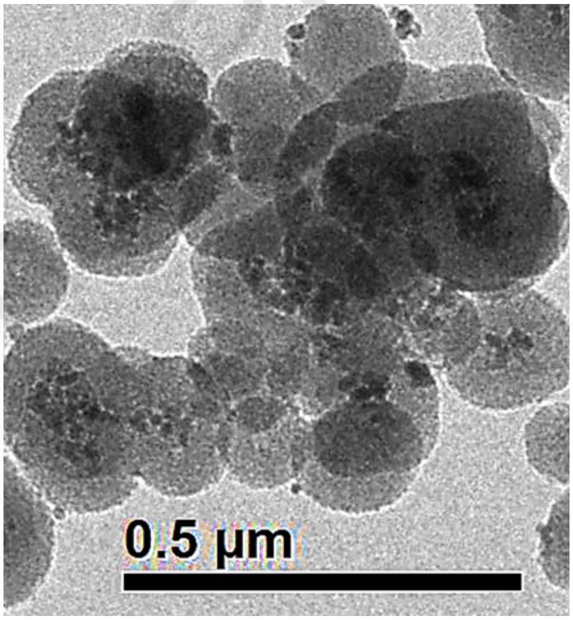

Fig. 5. TEM analysis of Mag@MCM-41/TiO_2

The VSM curve of Mag@MCM-41/TiO_2 nanocatalyst is presented in Fig. 6. As shown, the saturation magnetization for the material is 25 emu/g confirming good magnetic properties of this sample.

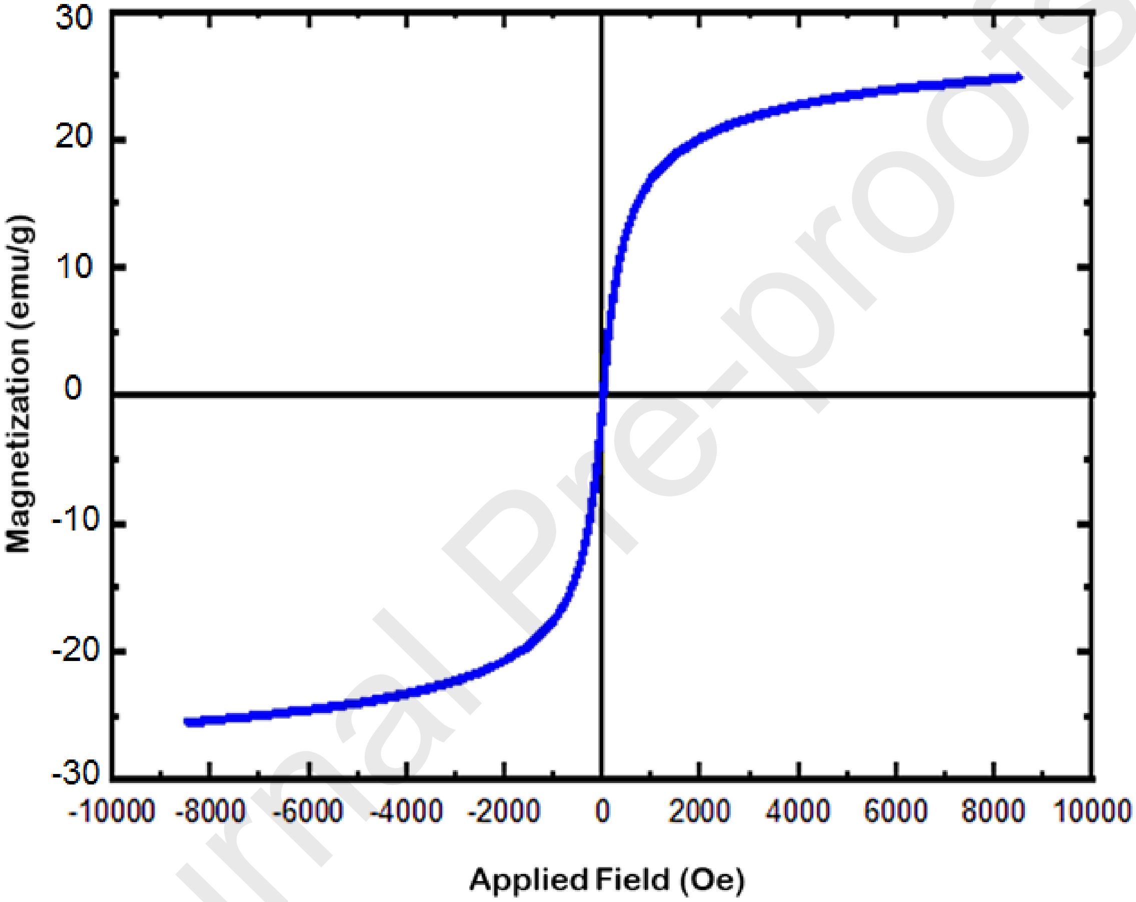

Fig. 6. VSM diagram of the Mag@MCM-41/TiO_2 nanocatalyst

After characterization of Mag@MCM-41/TiO_2 nanocatalyst, its catalytic application was investigated in the production of 1-(α-aminoalkyl)-2-naphthols (Scheme 2) under different conditions (Table 1). For this, the reaction between 2–naphthol, benzaldehyde and piperidine in the presence of Mag@MCM-41/TiO_2 in an ultrasonic bath was chosen as a test experiment. Firstly, the effect of catalyst loading in the reaction progress was studied. It was found that the existence of catalyst is essential for performing the reaction (Table 1, entry 1). The study of effect of catalyst loading showed that the best result is obtained in the presence of 2.3 mol% of Mag@MCM-41/TiO_2 (Table 1, entries 2-4). The temperature effect was also studied in the reaction progress that 50 °C was introduced as optimum (Table 1, entry 3 *versus* entries 5, 6). The solvent study showed that under solvent-free media the better result is obtained compared to water and ethanol solvents (Table 1, entry 3 *versus* entries 7, 8). In the next, the reaction progress was studied in an oil bath and the result was compared with that of ultrasonic bath (Table 1, entry 3 *versus* entry 9). Interestingly, both catalytic activity and product yield were better for ultrasonic media confirming the important role of ultrasonic waves in the progress of reaction that may be attributed to better dispersion of isolated catalytic nanoparticles under ultrasonic conditions. In another study, the catalytic activity of Ti-free Fe_3O_4 and Mag@MCM-41 materials in the model reaction was studied and the results were compared with those of present catalyst. Interestingly, under the same conditions as Mag@MCM-41/TiO_2, the Fe_3O_4 and Mag@MCM-41 delivered only 22 and 9% of desired product, respectively, confirming that the process is mainly catalyzed by supported Ti-species (Table 1, entry 3 *versus* entries 10, 11). According to these studies, 2.3 mol% of Mag@MCM-41/TiO_2 catalyst, 50 °C, solvent free conditions and ultrasonic irradiations were introduced as optimum conditions.

Table 1. Screening different parameters to prepare 1-(α-aminoalkyl)-2-naphthols

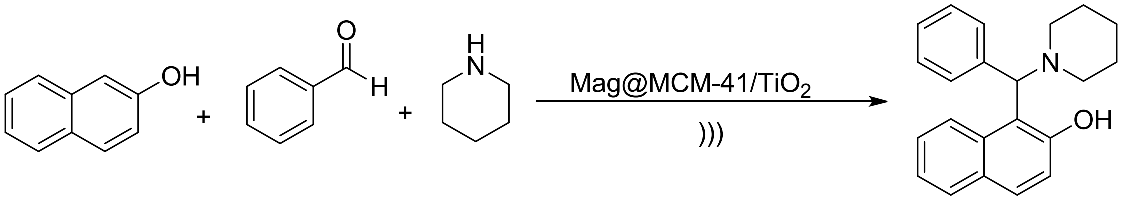

Entry	Solvent	Cat. (mol %)	T (°C)	Time (min)	Yield (%)[a]
1	---	---	50	60	---
2	---	1.36	50	60	90
3	**---**	**2.3**	**50**	**60**	**95**
4	---	3.19	50	60	95
5	---	2.3	r.t.	60	75
6	---	2.3	60	60	96
7	H_2O	2.3	50	60	70
8	EtOH	2.3	50	60	85
9[b]	---	2.3	50	60	73
10	---	Fe_3O_4 [c]	50	60	22
11	---	Mag@MCM-41 [d]	50	60	9

[a] Isolated yields. [b] The reaction was performed in an oil bath. [c] 0.005 g of Fe_3O_4 was used. [d] 0.005 g of Mag@MCM-41 was used.

After optimization of reaction conditions, various aldehydes were applied to prepare different 1-(α-aminoalkyl)-2-naphthols (Table 2). The results showed that both electron donating and electron withdrawing containing substituents afford their corresponding products in high yield and selectivity confirming high efficacy of this catalyst to prepare desired products. The other aromatic and aliphatic primary amines such as aniline and butanamine were also used as substrate delivering high yield of corresponding 1-(α-aminoalkyl)-2-naphthols. These data confirm high efficiency of designed catalyst in the synthesis different derivatives of Betti products.

Table 2. Production of 1-(α-aminoalkyl)-2-naphthols in the presence of Mag@MCM-41/TiO_2

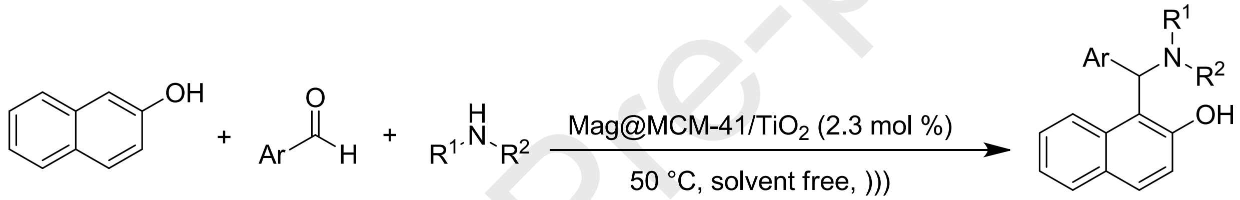

Entry	Ar	Amine	*t* (min)	Yield (%)[a]	Found M. P. (ºC)	Reported M. P. (°C)
1	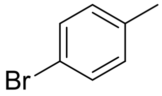	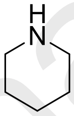	65	94	159-161	158-160 [48]
2	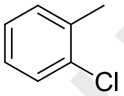	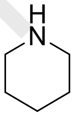	75	88	136-138	136-138 [48]
3	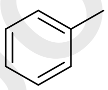	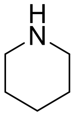	60	95	195-196	194-195 [49]
4	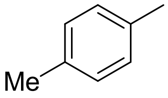	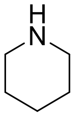	75	84	144-146	145-147 [49]

5	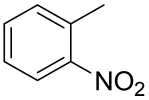	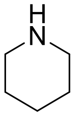	50	96	196-198	194-195 [49]
6	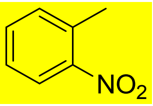	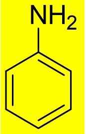	52	90	132-134	131.7-133.9 [39]
7	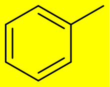	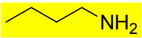	50	94	130-132	133-135 [40]

[a] Isolated yields.

Since the use of efficient heterogeneous catalysts in chemical industries has become increasingly important to reduce environmental pollution and production costs, in the next some experiments were carried out to study the recoverability and reusability of the Mag@MCM-41/TiO_2 catalyst. With this aim, after completion of the reaction, the Mag@MCM-41/TiO_2 was recovered and then reused under the same conditions as the first run. The procedure was repeated and the result demonstrated that the catalyst can be recovered and reapplied for at least seven times with no noticeable reduction in its activity (Fig. 7).

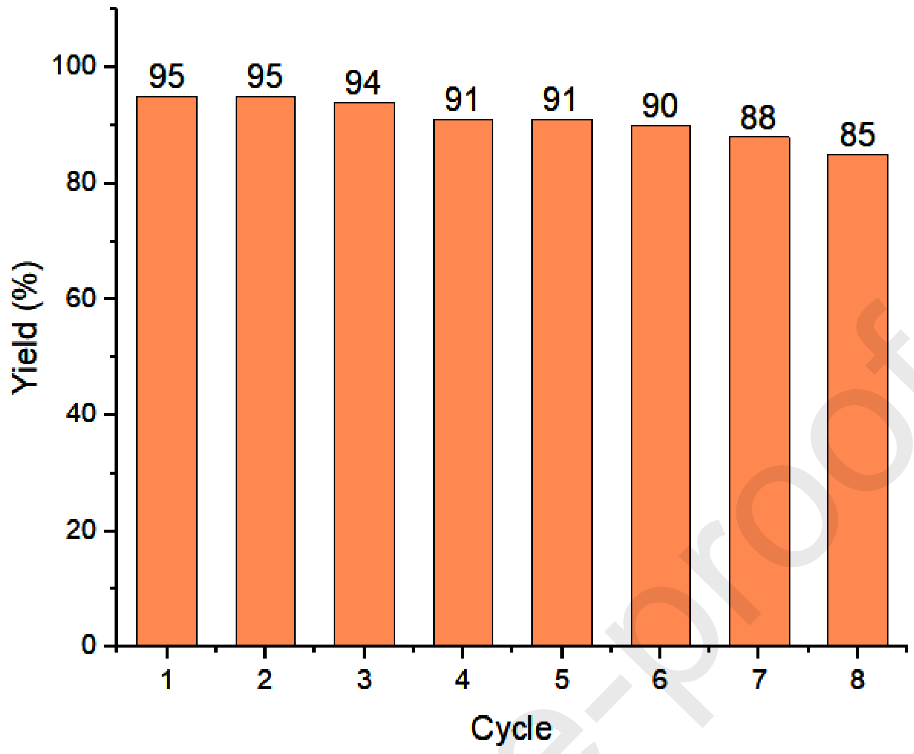

Fig. 7. Reusability of the Mag@MCM-41/TiO_2 nanocatalyst

In the next step, the leaching test was performed to prove heterogeneity behavior of catalyst. For this purpose, the reaction between 2–naphthol, benzaldehyde and piperidine in the presence of Mag@MCM-41/TiO_2 was selected as model reaction under the optimal conditions. After about 50 % progress of the reaction, the Mag@MCM-41/TiO_2 was removed by a magnet. Then, the reaction of residue was screened under optimal conditions. Interestingly, after 2 h, no significant conversion was observed confirming that the Mag@MCM-41/TiO_2 catalyst heterogeneously works under applied conditions.

Finally, the efficiency of Mag@MCM-41/TiO_2 catalyst was compared with the recently catalysts used in the synthesis of 1-(α-aminoalkyl)-2-naphthols (Table 3). The results showed that the present catalyst is more favorable than other catalysts, especially in terms of catalyst loading, yield and the number of recycling times.

Table 3. Comparative study of the efficiency of the present catalyst with that of previously reported catalytic systems

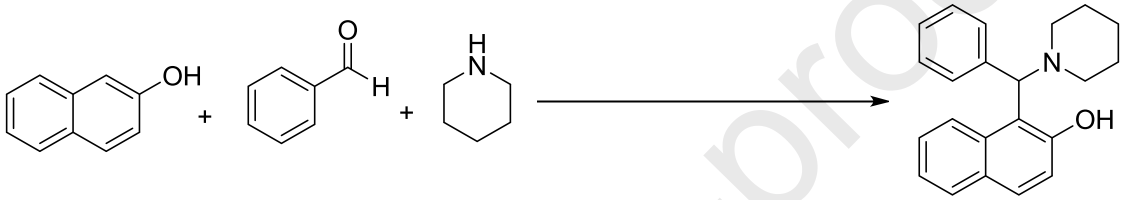

Catalyst	Conditions	Time	Yield (%)	Recovery times	Ref.
Non-ionic surfactants (Triton X-100)	Cat. 5 mol %, 25 ºC, H_2O	150	90	---	[38]
$Cu(OTf)_2.SiO_2$	Cat. 10 mol %, 40 ºC, neat	45	92	---	[36]
Nanocrystalline MgO	Cat. 50 mg, 25 ºC, H_2O	180	90	---	[35]
Fe_3O_4 MNPs	Cat. 0.1 g, 80 ºC, solvent-free,)))	25	90	6	[37]
Mag@MCM-41/TiO_2	Cat. 2.3 mol %, 50 ºC, solvent-free,)))	60	95	7	This work

4. Conclusion

In this paper, a novel Ti-containing core-shell material with magnetite core and nanoporous MCM-41 shell (Mag@MCM-41/TiO_2) was prepared, characterized and its catalytic application was studied in the synthesis of 1-(α-aminoalkyl)-2-naphthols. The VSM analysis showed magnetic good properties for Mag@MCM-41/TiO_2 nanocatalyst. The spherical morphology of this nanocatalyst was confirmed by using SEM and TEM analyses. The PXRD analysis proved high stability of crystalline Fe_3O_4 NPs during catalyst preparation. The Mag@MCM-41/TiO_2 was applied as an effective and powerful catalyst in the synthesis of 1-(α-aminoalkyl)-2-naphthols. The Mag@MCM-41/TiO_2 nanocatalyst was successfully recovered for seven times with no remarkable reduction in its activity. Other outstanding properties of this work were solvent free conditions, high reaction rate and no leaching of catalytic TiO_2 centers during reaction. According to the results obtained in this study, some applications of the present catalyst in other organic processes are underway in our laboratories.

Acknowledgments

The authors thank the Yasouj University and the Iran National Science Foundation (INSF) for supporting this work.

References

[1] A. Ali, M.Z. Hira Zafar, I. ul Haq, A.R. Phull, J.S. Ali, A. Hussain, Synthesis, characterization, applications, and challenges of iron oxide nanoparticles, Nanotechnol. Sci. Appl. 9 (2016) 49.

[2] Q. Zhai, B. Du, R. Feng, W. Xu, Q. Wei, A highly sensitive gas sensor based on Pd-doped Fe 3 O 4 nanoparticles for volatile organic compounds detection, Anal. Methods 6 (2014) 886.

[3] F. Zhang, T. Zhang, X. Yang, L. Zhang, K. Leng, Y. Huang, Y. Chen, A high-performance supercapacitor-battery hybrid energy storage device based on graphene-enhanced electrode materials with ultrahigh energy density, Energy Environ. Sci. 6 (2013) 1623.

[4] R.K. Sharma, S. Dutta, S. Sharma, R. Zboril, R.S. Varma, M.B. Gawande, Fe 3 O 4 (iron oxide)-supported nanocatalysts: synthesis, characterization and applications in coupling reactions, Green Chem. 18 (2016) 3184.

[5] T. Cheng, D. Zhang, H. Li, G. Liu, Magnetically recoverable nanoparticles as efficient catalysts for organic transformations in aqueous medium, Green Chem. 16 (2014) 3401.

[6] S. Chen, B. Bai, Y. He, N. Hu, H. Wang, Y. Suo, Controllable conversion of Prussian blue@ yeast bio-template into 3D cage-like magnetic Fe 3 O 4@ N-doped carbon absorbent and its cohesive regeneration by persulfate activation, RSC Adv. 9 (2019) 1151.

[7] Z. Wang, S. Zhai, J. Lv, H. Qi, W. Zheng, B. Zhai, Q. An, Versatile hierarchical Cu/Fe 3 O 4 nanocatalysts for efficient degradation of organic dyes prepared by a facile, controllable hydrothermal method, RSC Adv. 5 (2015) 74575.

[8] R. Das, C.D. Vecitis, A. Schulze, B. Cao, A.F. Ismail, X. Lu, J. Chen, S. Ramakrishna, Recent advances in nanomaterials for water protection and monitoring, Chem. Soc. Rev. 46 (2017) 6946.

[9] L. Zeng, W. Ren, L. Xiang, J. Zheng, B. Chen, A. Wu, Multifunctional Fe 3 O 4–TiO 2 nanocomposites for magnetic resonance imaging and potential photodynamic therapy, Nanoscale 5 (2013) 2107.

[10] D. Ni, W. Bu, E.B. Ehlerding, W. Cai, J. Shi, Engineering of inorganic nanoparticles as magnetic resonance imaging contrast agents, Chem. Soc. Rev. 46 (2017) 7438.

[11] R. Qiao, C. Yang, M. Gao, Superparamagnetic iron oxide nanoparticles: from preparations to in vivo MRI applications, J. Mater. Chem. 19 (2009) 6274.

[12] A.R.K. Sasikala, A. GhavamiNejad, A.R. Unnithan, R.G. Thomas, M. Moon, Y.Y. Jeong, C.H. Park, C.S. Kim, A smart magnetic nanoplatform for synergistic anticancer therapy: manoeuvring mussel-inspired functional magnetic nanoparticles for pH responsive anticancer drug delivery and hyperthermia, Nanoscale 7 (2015) 18119.

[13] J.B. Mamani, L.F. Gamarra, G.E.d.S. Brito, Synthesis and characterization of Fe3O4 nanoparticles with perspectives in biomedical applications, Mat. Res. 17 (2014) 542.

[14] S. Lian, Z. Kang, E. Wang, M. Jiang, C. Hu, L. Xu, Convenient synthesis of single crystalline magnetic Fe3O4 nanorods, Solid State Commun. 127 (2003) 605.

[15] K.G. Neoh, E.T. Kang, Surface modification of magnetic nanoparticles for stem cell labeling, Soft Matter 8 (2012) 2057.

[16] Y. Pan, X. Du, F. Zhao, B. Xu, Magnetic nanoparticles for the manipulation of proteins and cells, Chem. Soc. Rev. 41 (2012) 2912.

[17] M.S. Moorthy, Y. Oh, S. Bharathiraja, P. Manivasagan, T. Rajarathinam, B. Jang, T.T.V. Phan, H. Jang, J. Oh, Synthesis of amine-polyglycidol functionalised Fe 3 O 4@ SiO 2 nanocomposites for magnetic hyperthermia, pH-responsive drug delivery, and bioimaging applications, RSC Adv. 6 (2016) 110444.

[18] D. Yang, Z. Hou, Z. Cheng, C. Li, J. Lin, Current advances in lanthanide ion (Ln 3+)-based upconversion nanomaterials for drug delivery, Chem. Soc. Rev. 44 (2015) 1416.
[19] H.-X. Zhao, Q. Zou, S.-K. Sun, C. Yu, X. Zhang, R.-J. Li, Y.-Y. Fu, Theranostic metal–organic framework core–shell composites for magnetic resonance imaging and drug delivery, Chem. Sci. 7 (2016) 5294.
[20] S. Zeng, D. Baillargeat, H.-P. Ho, K.-T. Yong, Nanomaterials enhanced surface plasmon resonance for biological and chemical sensing applications, Chem. Soc. Rev. 43 (2014) 3426.
[21] K. Rout, M. Mohapatra, S. Layek, A. Dash, H. Verma, S. Anand, The influence of precursors on phase evolution of nano iron oxides/oxyhydroxides: optical and magnetic properties, New J. Chem. 38 (2014) 3492.
[22] J. Yue, X. Jiang, Y.V. Kaneti, A. Yu, Experimental and Theoretical Study of Low-Dimensional Iron Oxide Nanostructures, in: Smart Nanoparticles Technology, IntechOpen, 2012.
[23] W. Jiang, K.-L. Lai, H. Hu, X.-B. Zeng, F. Lan, K.-X. Liu, Y. Wu, Z.-W. Gu, The effect of [Fe 3+]/[Fe 2+] molar ratio and iron salts concentration on the properties of superparamagnetic iron oxide nanoparticles in the water/ethanol/toluene system, J. Nanoparticle Res. 13 (2011) 5135.
[24] W. Wu, C.Z. Jiang, V.A. Roy, Designed synthesis and surface engineering strategies of magnetic iron oxide nanoparticles for biomedical applications, Nanoscale 8 (2016) 19421.
[25] S. Wei, Q. Wang, J. Zhu, L. Sun, H. Lin, Z. Guo, Multifunctional composite core–shell nanoparticles, Nanoscale 3 (2011) 4474.
[26] J. Wang, Z.H. Shah, S. Zhang, R. Lu, Silica-based nanocomposites via reverse microemulsions: classifications, preparations, and applications, Nanoscale 6 (2014) 4418.
[27] S. Huang, L. Gu, N. Zhu, K. Feng, H. Yuan, Z. Lou, Y. Li, A. Shan, Heavy metal recovery from electroplating wastewater by synthesis of mixed-Fe 3 O 4@ SiO 2/metal oxide magnetite photocatalysts, Green Chem. 16 (2014) 2696.
[28] S. Wang, Z. Zhang, B. Liu, J. Li, Silica coated magnetic Fe 3 O 4 nanoparticles supported phosphotungstic acid: a novel environmentally friendly catalyst for the synthesis of 5-ethoxymethylfurfural from 5-hydroxymethylfurfural and fructose, Catal. Sci. Technol. 3 (2013) 2104.
[29] R. Hajian, A. Ehsanikhah, Manganese porphyrin immobilized on magnetic MCM-41 nanoparticles as an efficient and reusable catalyst for alkene oxidations with sodium periodate, Chem. Phys. Lett. 691 (2018) 146.
[30] M. Nikoorazm, F. Ghorbani, A. Ghorbani-Choghamarani, Z. Erfani, Pd (0)-S-propyl-2-aminobenzothioate immobilized onto functionalized magnetic nanoporous MCM-41 as efficient and recyclable nanocatalyst for the Suzuki, Stille and Heck cross coupling reactions, Appl. Organomet. Chem. 32 (2018) e4282.
[31] Y. Chen, S. Mu, Core–shell structured Fe3O4 nanoparticles functionalized with rhodamine derived probe for the detection, adsorption and removal of Hg (II): a sensing system with 'warning'signal, Sens Actuators B Chem 192 (2014) 275.
[32] F. Zhang, X. Wu, C. Liang, X. Li, Z. Wang, H. Li, Highly active, water-compatible and easily separable magnetic mesoporous Lewis acid catalyst for the Mukaiyama–Aldol reaction in water, Green Chem. 16 (2014) 3768.
[33] A. Ulu, S.A.A. Noma, S. Koytepe, B. Ates, Magnetic Fe3O4@ MCM-41 core–shell nanoparticles functionalized with thiol silane for efficient l-asparaginase immobilization, Artif Cells Nanomed Biotechnol (2018) 1.
[34] F. Hoffmann, M. Cornelius, J. Morell, M. Fröba, Silica-based mesoporous organic–inorganic hybrid materials, Angew. Chem. Int. Ed. 45 (2006) 3216.
[35] B. Karmakar, J. Banerji, A competent pot and atom-efficient synthesis of Betti bases over nanocrystalline MgO involving a modified Mannich type reaction, Tetrahedron Lett. 52 (2011) 4957.

[36] S.D. Dindulkar, V.G. Puranik, Y.T. Jeong, Supported copper triflate as an efficient catalytic system for the synthesis of highly functionalized 2-naphthol Mannich bases under solvent free condition, Tetrahedron Lett. 53 (2012) 4376.

[37] M. Mokhtary, M. Torabi, Nano magnetite (Fe3O4), an efficient and robust catalyst for the one-pot synthesis of 1-(aryl (piperidin-1-yl) methyl) naphthalene-2-ol and 1-(α-amido alkyl)-2-naphthol under ultrasound irradiation, J. Saudi Chem. Soc. 21 (2017) S299.

[38] A. Kumar, M.K. Gupta, M. Kumar, Non-ionic surfactant catalyzed synthesis of Betti base in water, Tetrahedron Lett. 51 (2010) 1582.

[39] J. Mou, G. Gao, C. Chen, J. Liu, J. Gao, Y. Liu, D. Pei, Highly efficient one-pot three-component Betti reaction in water using reverse zinc oxide micelles as a recoverable and reusable catalyst, RSC Adv. 7 (2017) 13868.

[40] S. Fathalipour, B. Ataei, F. Janati, Aqueous suspension of biocompatible reduced graphene oxide-Au NPs composite as an effective recyclable catalyst in a Betti reaction, Mater. Sci. Eng. C 97 (2019) 356.

[41] R. Teimuri-Mofrad, M. Gholamhosseini-Nazari, S. Esmati, A. Shahrisa, An efficient and green method for the synthesis of Betti base employing nano-SiO 2–H 3 BO 3 as a novel recyclable heterogeneous catalyst, Res. Chem. Intermed. 43 (2017) 6845.

[42] B.L. Gadilohar, H.S. Kumbhar, G.S. Shankarling, Choline peroxydisulfate oxidizing Bio-TSIL: triple role player in the one-pot synthesis of Betti bases and gem-bisamides from aryl alcohols under solvent-free conditions, New J. Chem. 39 (2015) 4647.

[43] A.H. Fernandez, R.M. Alvarez, T.M. Abajo, Improved Synthesis of Symmetrical N, N'-Alkylidene Bisamides, Synthesis 1996 (1996) 1299.

[44] A. Zare, S. Akbarzadeh, E. Foroozani, H. Kaveh, A.R. Moosavi-Zare, A. Hasaninejad, M. Mokhlesi, M.H. Beyzavi, M.A. Zolfigol, Triethylamine-bonded sulfonic acid ([Et 3N–SO 3H] Cl): a highly efficient and homogeneous catalyst for the condensation of 2-naphthol with arylaldehydes and amides (alkyl carbamates or thioamides), J. Sulfur Chem. 33 (2012) 259.

[45] A. Kumar, M.S. Rao, V.K. Rao, Sodium Dodecyl Sulfate-assisted Synthesis of 1-(Benzothiazolylamino) methyl-2-naphthols in Water, Aust. J. Chem. 63 (2010) 1538.

[46] Z. Ramazani, D. Elhamifar, M. Norouzi, R. Mirbagheri, Magnetic mesoporous MCM-41 supported boric acid: A novel, efficient and ecofriendly nanocomposite, Composites: Part B 164 (2019) 10.

[47] D. Elhamifar, P. Mofatehnia, M. Faal, Magnetic nanoparticles supported Schiff-base/copper complex: An efficient nanocatalyst for preparation of biologically active 3, 4-dihydropyrimidinones, J. Colloid Interface Sci. 504 (2017) 268.

[48] C. Mukhopadhyay, S. Rana, R.J. Butcher, Catalyst-free, one-pot, expeditious synthesis of aminoalkylnaphthols at room temperature, Synth. Commun. 42 (2012) 3077.

[49] A. Jha, N.K. Paul, S. Trikha, T.S. Cameron, Novel synthesis of 2-naphthol Mannich bases and their NMR behaviour, Can. J. Chem. 84 (2006) 843.

[50] R. Wang, X. Wang, X. Xi, R. Hu, G. Jiang, Preparation and photocatalytic activity of magnetic Fe3O4/SiO2/TiO2 composites, Adv. Mater. Sci. Eng. 2012 (2012).

Graphical abstract:

A novel magnetic ordered mesoporous silica-titania (Mag@MCM-41/TiO_2) material with core-shell structure was synthesized, characterized and its catalytic application was investigated in Betti reaction.

Marziyeh Vahidian, Dawood Elhamifar* and Masoumeh Shaker

Department of Chemistry, Yasouj University, Yasouj, 75918-74831, Iran

E-mail: d.elhamifar@yu.ac.ir